

Controlling Canard Cycles

Hildeberto Jardón-Kojakhmetov and Christian Kuehn

May 2, 2022

Abstract

Canard cycles are periodic orbits that appear as special solutions of fast-slow systems (or singularly perturbed Ordinary Differential Equations). It is well known that canard cycles are difficult to detect, hard to reproduce numerically, and that they are sensible to exponentially small changes in parameters. In this paper we combine techniques from geometric singular perturbation theory, the blow-up method, and control theory, to design controllers that stabilize canard cycles of planar fast-slow systems with a folded critical manifold. As an application, we propose a controller that produces stable mixed-mode oscillations in the van der Pol oscillator.

1 Introduction

Fast-slow systems (also known as singularly perturbed ordinary differential equations, see more details in Section 2) are often used to model phenomena occurring in two or more time scales. Examples of these are vast and range from oscillatory patterns in biochemistry and neuroscience [17, 25, 6, 24], all the way to stability analysis and control of power networks [10, 13], among many others [40, Chapter 20]. The overall idea behind the analysis of fast-slow systems is to separate the behavior that occurs at each time scale, understand such behavior, and then try to elucidate the corresponding dynamics of the full system. Many approaches have been developed, such as asymptotic methods [16, 33, 50, 51], numeric and computational tools [23, 31], and geometric techniques [19, 30, 32], see also [40, 45, 55]. In this article we take a geometric approach.

Although the time scale separation approach has been very fruitful, there are some cases in which it does not suffice to completely describe the dynamics of a fast-slow system, see the details in Section 2. The reason is that, for some systems, the fast and the slow dynamics are interrelated in such a way that some complex behavior is only discovered when they are not fully separated. An example of the aforementioned situation are the so-called *canards* [7, 8, 14], see Section 2.1 for the appropriate definition. Canards are orbits that, counter-intuitively, stay close for a considerable amount of time to a repelling set of equilibrium points of the fast dynamics. Canards are extremely important not only in the theory of fast-slow systems, but also in applied sciences, and especially in neuroscience, as they have allowed, for example, the detailed description of the very fast onset of large amplitude oscillations due to small changes of a parameter in neuronal models [17, 25] and of other complex oscillatory patterns [9, 11, 46]. Due to their very nature, canard orbits are not robust, meaning that small perturbations may drastically change the shape of the orbit.

On the other hand the application of singular perturbation techniques in control theory is far-reaching. Perhaps, as already introduced above, one of the biggest appeals of the theory of fast-slow systems is the time scale separation, which allows the reduction of large systems into

lower dimensional ones for which the control design is simpler [28, 37, 36]. Applications range from the control of robots [52, 53, 27], all the way to industrial biochemical processes, and large power networks [12, 34, 35, 42, 49, 48]. However, as already mentioned, not all fast-slow systems can be analyzed by the convenient time scale separation strategy, and although some efforts from very diverse perspectives have been made [2, 3, 4, 5, 21, 22, 28, 29], a general theory that includes not only the regulation problem but also the path following and trajectory planning problems is, to date, lacking.

The main goal of this article is to merge techniques of fast-slow dynamical systems with control theory methods to develop controllers that stabilize canard orbits. The idea of controlling canards has already been explored in [15], where an integral feedback controller is designed for the FitzHugh-Nagumo model to steer it towards the so-called “canard regime”. In contrast, here we take a more general and geometric approach by considering the canard normal form, see Section 2.1. Moreover, we integrate control techniques with Geometric Singular Perturbation Theory (GSPT) and propose a controller design methodology in the blow-up space. Later we apply such geometric insight to the van der Pol oscillator where we provide a controller that produces any oscillatory pattern allowed by the geometric properties of the model, see Section 4.

The rest of this document is arranged as follows: in Section 2 we present definitions and preliminaries of the geometric theory of fast-slow systems and of canards, which are necessary for the main analysis. In Section 3 we develop a controller that stabilizes folded canard orbits, where the main strategy is to combine the blow-up method with state-feedback control techniques to achieve the goal. Afterwards in Section 4, as an extension to our previously developed controller, we develop a controller that stabilizes several canard cycles and is able to produce robust complex oscillatory patterns in the van der Pol oscillator. We finish in Section 5 with some concluding remarks and an outlook.

2 Preliminaries

A fast-slow system is a singularly perturbed ordinary differential equation (ODE) of the form

$$\begin{aligned}\varepsilon \dot{x} &= f(x, y, \varepsilon, \lambda) \\ \dot{y} &= g(x, y, \varepsilon, \lambda),\end{aligned}\tag{1}$$

where $x \in \mathbb{R}^m$ is the *fast variable*, $y \in \mathbb{R}^n$ the *slow variable*, $0 < \varepsilon \ll 1$ is a small parameter accounting for the time scale separation between the aforementioned variables, $\lambda \in \mathbb{R}^p$ denotes other parameters, and f and g are assumed sufficiently smooth. Along this document the over-dot is used to denote the derivative with respect to the *slow* time τ . It is well-known that, for $\varepsilon > 0$, an equivalent way of writing (1) is

$$\begin{aligned}x' &= f(x, y, \varepsilon, \lambda) \\ y' &= \varepsilon g(x, y, \varepsilon, \lambda),\end{aligned}\tag{2}$$

where now the prime denotes the derivative with respect to the *fast* time $t := \tau/\varepsilon$.

One of the mathematical theories that is concerned with the analysis of (1)-(2) is Geometric Singular Perturbation Theory (GSPT) [40]. The overall idea of GSPT is to study the limit equations that result from setting $\varepsilon = 0$ in (1)-(2). Then, one looks for invariant objects that can be shown

to persist up to small perturbations. Such invariant objects give a qualitative description of the behavior of (1)-(2). Accordingly, setting $\varepsilon = 0$ in (1)-(2) one gets

$$\begin{aligned} 0 &= f(x, y, 0, \lambda) & x' &= f(x, y, 0, \lambda) \\ \dot{y} &= g(x, y, 0, \lambda) & y' &= 0, \end{aligned} \tag{3}$$

known, respectively, as the *reduced slow subsystem* (which is a Constrained Differential Equation [54] or a Differential Algebraic Equation [41]) and *the layer equation*. The aforementioned limit systems are not equivalent any more, but they are related by the following important geometric object.

Definition 1 (The critical manifold). *The critical manifold is defined as*

$$\mathcal{C}_0 = \{(x, y) \in \mathbb{R}^m \times \mathbb{R}^n \mid f(x, y, 0, \lambda) = 0\}. \tag{4}$$

We note that the critical manifold is the phase-space of the reduced slow subsystem and the set of equilibrium points of the layer equation. The properties of the critical manifold are essential to GSPT, in particular the following.

Definition 2 (Normal hyperbolicity). *Let $p \in \mathcal{C}_0$. We say that p is hyperbolic if the matrix $D_x f(x, y, 0, \lambda)|_{\mathcal{C}_0}$ has all its eigenvalues away from the imaginary axis. If every point $p \in \mathcal{C}_0$ is hyperbolic, we say that \mathcal{C}_0 is normally hyperbolic. On the contrary, if for some $p \in \mathcal{C}_0$ the matrix $D_x f(x, y, 0, \lambda)|_{\mathcal{C}_0}$ has at least one of its eigenvalues on the imaginary axis, then we say that p is a non-hyperbolic point.*

It is known from Fenichel's theory [18, 19] that a *compact and normally hyperbolic* critical manifold $\mathcal{S}_0 \subseteq \mathcal{C}_0$ of (3) persists as a locally invariant *slow* manifold \mathcal{S}_ε under sufficiently small perturbations. In other words, Fenichel's theory guarantees that in a neighborhood of a normally hyperbolic critical manifold the dynamics of (1)-(2) are well approximated by the limit systems (3).

Remark 1. *Along this paper we use the notation \mathcal{S}_0^a and \mathcal{S}_0^r to denote, depending on the eigenvalues of $D_x f(x, y, 0, \lambda)|_{\mathcal{S}_0}$, the attracting and repelling parts of the (compact) critical manifold \mathcal{S}_0 . Accordingly, the corresponding slow manifolds are denoted as $\mathcal{S}_\varepsilon^a$ and $\mathcal{S}_\varepsilon^r$.*

On the other hand, critical manifolds may lose normal hyperbolicity, for example, due to singularities of the layer equation, see Figure 1. It is in fact due to loss of normal hyperbolicity that, as in this paper, some interesting and complicated dynamics may arise in seemingly simple fast-slow systems. Fenichel's theory, however, does not hold in the vicinity of non-hyperbolic points. In some cases, depending on the nature of the non-hyperbolicity, the *blow-up method* [26] is a suitable technique to analyze the complicated dynamics that arise. In the forthcoming section we introduce the particular type of orbits that we are concerned with and that arise due to loss of normal-hyperbolicity of the critical manifold; the so-called *canards*.

2.1 Canards

To keep this section as concise as possible, we are going to present canards and in particular canard cycles in its most well-known setting. The interested reader is referred to, e.g. [14, 38, 56], references therein and, in particular, [40, Chapter 8] and [26, Section 3] for more detailed information.

Let us start by recalling that the canonical form of a canard point [38] is given by

$$\begin{aligned} x' &= -yh_1(x, y, \varepsilon, \alpha) + x^2h_2(x, y, \varepsilon, \alpha) + \varepsilon h_3(x, y, \varepsilon, \alpha) \\ y' &= \varepsilon (xh_4(x, y, \varepsilon, \alpha) - \alpha h_5(x, y, \varepsilon, \alpha) + yh_6(x, y, \varepsilon, \alpha)), \end{aligned} \quad (5)$$

where $(x, y) \in \mathbb{R}^2$, $0 < \varepsilon \ll 1$, and $\alpha \in \mathcal{O}(1)$ is assumed to be a small parameter. Furthermore

$$\begin{aligned} h_3(x, y, \varepsilon, \alpha) &= \mathcal{O}(x, y, \varepsilon, \alpha) \\ h_i(x, y, \varepsilon, \alpha) &= 1 + \mathcal{O}(x, y, \varepsilon, \alpha), \quad i = 1, 2, 4, 5, \end{aligned} \quad (6)$$

and h_6 is smooth. For simplicity of notation, we rewrite (5) together with (6) as

$$\begin{aligned} x' &= -y + x^2 + \tilde{f}(x, y, \varepsilon, \alpha) \\ y' &= \varepsilon(x - \alpha + \tilde{g}(x, y, \varepsilon, \alpha)), \end{aligned} \quad (7)$$

where

$$\begin{aligned} \tilde{f}(x, y, \varepsilon, \alpha) &:= (-y + x^2 + \varepsilon)\mathcal{O}(x, y, \varepsilon, \alpha) \\ \tilde{g}(x, y, \varepsilon, \alpha) &:= (x - \alpha)\mathcal{O}(x, y, \varepsilon, \alpha) + yh_6(x, y, \varepsilon, \alpha). \end{aligned} \quad (8)$$

The critical manifold is locally (near the origin) a parabola and is given by

$$\mathcal{S}_0 = \left\{ (x, y) \in \mathbb{R}^2 \mid -y + x^2 + \tilde{f}(x, y, 0, \alpha) = 0 \right\}. \quad (9)$$

The (slow and fast) reduced flow corresponding to (7) is as shown in Figure 1.

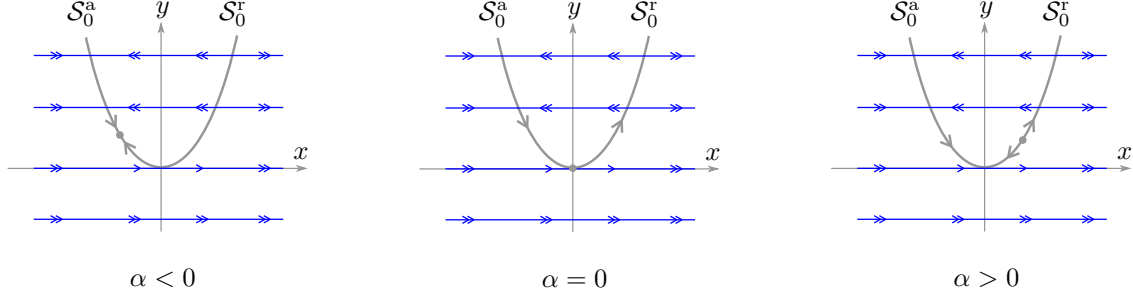


Figure 1: Singular flow of (7) near the origin. The grey parabola depicts the critical manifold \mathcal{S}_0 which is partitioned in its attracting $\mathcal{S}_0^a = \mathcal{S}_0|_{\{x < 0\}}$ and repelling $\mathcal{S}_0^r = \mathcal{S}_0|_{\{x > 0\}}$ parts, while the origin (the fold point) is non-hyperbolic. If $\alpha = 0$ the origin is also called *canard point*. In this latter case, the orbit along the critical manifold is also known as *singular maximal canard*.

Remark 2. To fix ideas, consider for a moment (7) with zero higher order terms¹, that is

$$\begin{aligned} x' &= -y + x^2 \\ y' &= \varepsilon(x - \alpha). \end{aligned} \quad (10)$$

¹Refer to [38] for the much more complicated case that includes the higher order terms.

Then, it is straightforward to check that, for $\varepsilon > 0$ and $\alpha = 0$, the orbits of (10) are given by level sets of

$$H(x, y, \varepsilon) = \frac{1}{2} \exp\left(-\frac{2y}{\varepsilon}\right) \left(\frac{y}{\varepsilon} - \frac{x^2}{\varepsilon} + \frac{1}{2}\right). \quad (11)$$

Some orbits of (10) are shown in Figure 2.

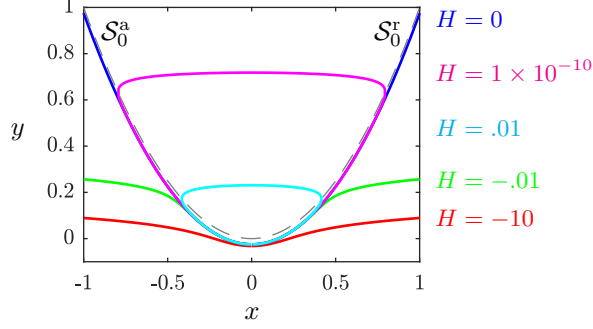


Figure 2: Orbits of (10) obtained as level sets of (11). The dashed grey curve is the critical manifold. Compare with $\alpha = 0$ in Figure 1.

What is remarkable is that there are orbits that closely follow the unstable branch of the critical manifold for slow time of order $\mathcal{O}(1)$. Such type of orbits are known as *canards*. There is a particular canard, which is called *maximal canard* and is given by $\{H = 0\}$ that connects the attracting slow manifold $\mathcal{S}_\varepsilon^a$ with the repelling one $\mathcal{S}_\varepsilon^r$. More relevant to this paper are periodic orbits with canard portions, which called *canard cycles*.

In the following section we design feedback controllers for (5) that render a particular canard cycle asymptotically stable. In other words, we consider the path following control problem where a canard orbit is the reference.

3 Controlling Folded Canards

We propose to study two control problems, namely

$$\begin{aligned} x' &= -y + x^2 + \tilde{f}(x, y, \varepsilon, \alpha) + u(x, y, \varepsilon, \alpha) \\ y' &= \varepsilon(x - \alpha + \tilde{g}(x, y, \varepsilon, \alpha)), \end{aligned} \quad (12)$$

which we call *the fast control problem* and

$$\begin{aligned} x' &= -y + x^2 + \tilde{f}(x, y, \varepsilon, \alpha) \\ y' &= \varepsilon(x - \alpha + \tilde{g}(x, y, \varepsilon, \alpha) + u(x, y, \varepsilon, \alpha)), \end{aligned} \quad (13)$$

to be referred to as *the slow control problem*. Recall that \tilde{f} and \tilde{g} stand for the higher order terms as in (8). The objective is to stabilize a certain reference canard cycle to be denoted by γ_h .

Remark 3.

- The choice of the above control problems is motivated by applications, especially in neuron models, see [15, 25, 17], where the input current appears in the fast (voltage) variable and regulates the distinct firing patterns. However, if one is interested in the fully actuated case, a combination of the techniques presented here shall also be useful.
- Throughout this document we assume that one has full knowledge of the functions \tilde{f} and \tilde{g} . This means that for the fast (resp. slow) control problem we assume $\tilde{f} = 0$ (resp. $\tilde{g} = 0$). Otherwise one considers a controller of the form $u = -\tilde{f} + v$ (resp. $u = -\tilde{g} + v$) where now v is to be designed.

Since we are going to use the blow-up method to design the controller, one should be aware that the controller may change the singularity being analysed. This motivates the following definition.

Definition 3 (Blow-up compatible controller). *Consider a control system*

$$\dot{\zeta} = f(\zeta, \lambda, u), \quad (14)$$

where $\zeta \in \mathbb{R}^n$ is the state variable, $\lambda \in \mathbb{R}^p$ denotes system parameters (possibly including $0 < \varepsilon \ll 1$) and $u \in \mathbb{R}^m$ stands for the controller. Suppose that for the open-loop system, that is when $u = 0$, the origin $\zeta = 0 \in \mathbb{R}^n$ is a nilpotent equilibrium point of $\dot{\zeta} = f(\zeta, 0, 0)$. Let u be a state-feedback controller, that is $u = u(\zeta, \eta)$, where $\eta \in \mathbb{R}^q$ are controller parameters and denote by $\dot{\zeta} = F(\zeta, \lambda, \eta)$ the closed-loop system. We say that u is a blow-up compatible controller if the functions $f(\zeta, 0, 0)$ and $F(\zeta, 0, 0)$ are germ-equivalent, that is, they define the same germ at the origin [1].

As an example of the above definition, recall that a planar fast-slow system with a generic fold at the origin is given by

$$\begin{aligned} x' &= f(x, y, \varepsilon) \\ y' &= \varepsilon g(x, y, \varepsilon), \end{aligned} \quad (15)$$

with $f(0, 0, 0) = 0$, $\frac{\partial f}{\partial x}(0, 0, 0) = 0$, $\frac{\partial^2 f}{\partial x^2}(0, 0, 0) \neq 0$, and $\frac{\partial f}{\partial y}(0, 0, 0) \neq 0$. Next, let $u = u(x, y, \varepsilon, \eta)$ be a state-feedback controller and suppose one considers the fast-slow control system

$$\begin{aligned} x' &= \underbrace{f(x, y, \varepsilon) + u(x, y, \varepsilon, \eta)}_{=: F(x, y, \varepsilon, \eta)} \\ y' &= \varepsilon g(x, y, \varepsilon). \end{aligned} \quad (16)$$

Then, u is blow-up compatible if $F(0, 0, 0) = 0$, $\frac{\partial F}{\partial x}(0, 0, 0) = 0$, $\frac{\partial^2 F}{\partial x^2}(0, 0, 0) \neq 0$, and $\frac{\partial F}{\partial y}(0, 0, 0) \neq 0$, which means that the controller does not change the class of the singularity.

3.1 The fast control problem

In this section we study the control problem defined by

$$\begin{aligned} x' &= -y + x^2 + u(x, y, \varepsilon, \alpha) \\ y' &= \varepsilon(x - \alpha + \tilde{g}(x, y, \varepsilon, \alpha)). \end{aligned} \quad (17)$$

Due to the fact that the slow dynamics are not actuated, we are going to stabilize canards centered at $(x, y) = (\alpha, 0)$. Then, it is convenient to define $\hat{x} = x - \alpha$, which brings (17) into

$$\begin{aligned}\hat{x}' &= -y + (\hat{x} + \alpha)^2 + \hat{u}(\hat{x}, y, \varepsilon, \alpha) \\ y' &= \varepsilon(\hat{x} + \hat{g}(\hat{x}, y, \varepsilon, \alpha)),\end{aligned}\tag{18}$$

where $\hat{u}(\hat{x}, y, \varepsilon, \alpha) = u(\hat{x} + \alpha, y, \varepsilon, \alpha)$ and similarly for \hat{g} .

Theorem 1. *Consider (18) and let $\hat{H} = H(\hat{x}, y, \varepsilon)$ be defined by (11). Then, the following hold:*

1. *One can choose constants $c_1 > 0$, $c_2 \in \mathbb{R}$ and $h \leq \frac{1}{4}$ such that the blow-up compatible controller*

$$\hat{u} = -2\alpha\hat{x} - \alpha^2 + c_1\hat{x}\varepsilon^{1/2}\exp(c_2y\varepsilon^{-1})(\hat{H} - h)\tag{19}$$

renders the canard orbit $\hat{\gamma}_h = \{(\hat{x}, y) \in \mathbb{R}^2 \mid \hat{H} = h\}$ locally asymptotically stable for $\varepsilon > 0$ sufficiently small.

2. *Let $\hat{\Gamma} \subset \mathbb{R}^2$ be a neighbourhood of $\hat{\gamma}_h$ for $h \in (0, \frac{1}{4})$. Suppose that, additionally to (8), \hat{g} is of the form $\hat{g} = \hat{x}\hat{\phi}(\hat{x}, y, \varepsilon, \alpha)$ for some smooth function $\hat{\phi}$, and that $\hat{\phi} > -1$ for all $(\hat{x}, y) \in \hat{\Gamma}$. Then one can choose constants $c_1 > 0$, $c_2 \in \mathbb{R}$ such that the blow-up compatible controller*

$$\hat{u} = -2\alpha\hat{x} - \alpha^2 + c_1\hat{x}\varepsilon^{1/2}(\hat{H} - h)\exp(c_2y\varepsilon^{-1}) - \varepsilon^{1/2}(y - \hat{x}^2)\hat{\phi}\tag{20}$$

renders the canard orbit $\hat{\gamma}_h = \{(\hat{x}, y) \in \mathbb{R}^2 \mid \hat{H} = h\}$ locally asymptotically stable.

3. *A convenient choice of gain c_2 for following the maximal canard ($h = 0$) is $c_2 \leq 2 + \frac{3}{2}\frac{\varepsilon}{y} \ln\left(K\frac{\varepsilon}{y}\right)$, for some $K > 0$. By convenient we mean that such choice ensures that, for $\alpha = 0$, the controller remains bounded as $y \rightarrow \infty$.*

The proof of Theorem 1 follows from the forthcoming analysis and is summarized in section 3.1.3. We show in Figure 3 a simulation of the results contained in Theorem 1.

As already anticipated, the idea is to design the controller \hat{u} in the blow-up space. Therefore, let us consider a coordinate transformation defined by

$$\hat{x} = \bar{r}\bar{x}, \quad y = \bar{r}^2\bar{y}, \quad \varepsilon = \bar{r}^2\bar{\varepsilon}, \quad \hat{u} = \bar{r}^2\bar{\mu}, \quad \alpha = \bar{r}\bar{\alpha},\tag{21}$$

where $(\bar{x}, \bar{y}, \bar{\varepsilon}, \bar{\mu}, \bar{\alpha}) \in \mathbb{S}^4$ and $\bar{r} \in [0, \infty)$. Analogous to the analysis of the canard point in [38] we consider the charts

$$\begin{aligned}K_1 : \quad \hat{x} &= r_1x_1, \quad y = r_1^2, \quad \varepsilon = r_1^2\varepsilon_1, \quad \hat{u} = r_1^2\mu_1, \quad \alpha = r_1\alpha_1, \\ K_2 : \quad \hat{x} &= r_2x_2, \quad y = r_2^2y_2, \quad \varepsilon = r_2^2, \quad \hat{u} = r_2^2\mu_2, \quad \alpha = r_2\alpha_2.\end{aligned}\tag{22}$$

The coordinates in the above charts are related by the *transition maps*:

$$\kappa_{12} : K_1 \rightarrow K_2, \quad r_2 = r_1\varepsilon_1^{1/2}, \quad x_2 = x_1\varepsilon_1^{-1/2}, \quad y_2 = \varepsilon_1^{-1}, \quad \mu_2 = \mu_1\varepsilon_1^{-1}, \quad \alpha_2 = \alpha_1\varepsilon_1^{-1/2},\tag{23}$$

for $\varepsilon_1 > 0$ and

$$\kappa_{21} : K_2 \rightarrow K_1, \quad r_1 = r_2y_2^{1/2}, \quad x_1 = x_2y_2^{-1/2}, \quad \mu_1 = \mu_2y_2^{-1}, \quad \varepsilon_1 = y_2^{-1}, \quad \alpha_1 = \alpha_2y_2^{-1/2},\tag{24}$$

for $y_2 > 0$.

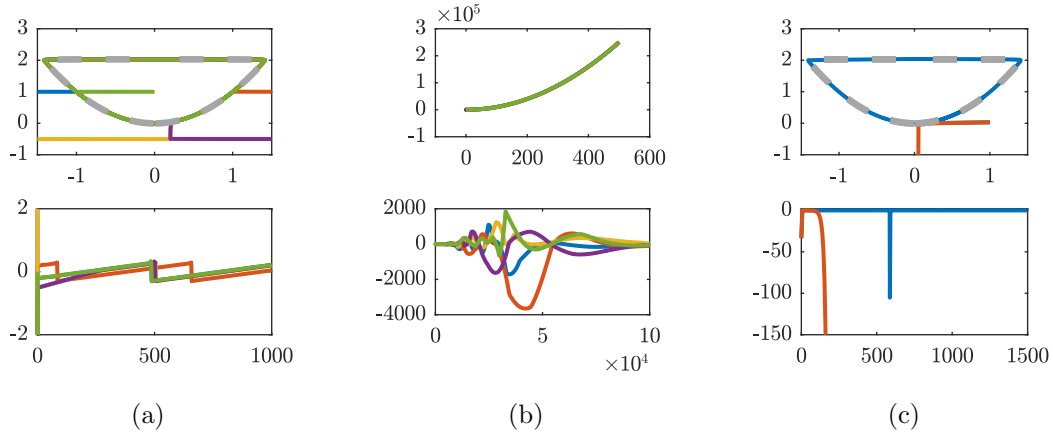


Figure 3: In all three columns we show, in the first row the (\hat{x}, y) phase portrait of the closed-loop system (18) and in the second row the time-series of the corresponding controller. In all these simulations $\varepsilon = 0.01$. (a) The case for which $\hat{g} = 0$ and with parameters $(\alpha, c_1, c_2, h) = (-0.1, 1, 2, \frac{1}{4}e^{-400})$. We remark here that in order for the constant $h = \frac{1}{4}e^{-400}$ to be numerically feasible one has to input $h \exp(c_2 y \varepsilon^{-1}) = \frac{1}{4} \exp(c_2 y \varepsilon^{-1} - 400)$ into the algorithm. The desired canard cycle to be followed is shown in dashed-gray. (b) The maximal canard case with $\hat{g} = 0$ and with parameters $(\alpha, c_1, c_2, h) = (0, 1, 2 - e^{-15}, 0)$. (c) An example of the effect of the extra term in (20) where we show two trajectories with the same initial conditions. The unstable one is obtained with the controller (19) while the stable one with (20). The desired canard cycle to be followed is shown in dashed-gray. The large spike in the controller is observed every time the trajectory crosses the y -axis long a fast fibre. For such simulation we have used $(\alpha, c_1, c_2, h) = (0, 5, 2, \frac{1}{4}e^{-400})$ and $g = 100x(y - x^2)$. For more details see Sections 3.1.1 and 3.1.2.

3.1.1 Analysis in the rescaling chart K_2

The blown-up (and desingularized) local vector field in this chart reads as

$$\begin{aligned} x'_2 &= -y_2 + (x_2 + \alpha_2)^2 + \mu_2 \\ y'_2 &= x_2 + r_2 g_2, \end{aligned} \quad (25)$$

where $g_2 = g_2(r_2, x_2, y_2, \alpha_2)$ is smooth and defined by the blow-up of \hat{g} . More precisely one has

$$g_2 = x_2 \mathcal{O}(x_2 + \alpha_2, y_2, r_2, \alpha_2) + y_2 \bar{h}_6(x_2, y_2, r_2, \alpha_2), \quad (26)$$

where \bar{h}_6 is smooth (recall (8)). Similarly, $\mu_2 = \mu_2(x_2, y_2, r_2, \alpha_2)$ is the blown-up state-feedback controller to be designed. Observe that, analogously to what is described in Remark 2, we have that for $r_2 = \alpha_2 = \mu_2 = 0$ the orbits of (25) are given as level sets of the function

$$H_2(x_2, y_2) = \frac{1}{2} \exp(-2y_2) \left(y_2 - x_2^2 + \frac{1}{2} \right). \quad (27)$$

Having this in mind, we are going to design μ_2 in such a way that for a trajectory $(x_2(t_2), y_2(t_2))$ of (25) one has $\lim_{t_2 \rightarrow \infty} H_2(x_2(t_2), y_2(t_2)) \rightarrow h$, where h defines the desired canard cycle and t_2 denotes the time-parameter of (25).

We approach the design of μ_2 as follows: we start by restricting to $\{r_2 = 0\}$ and define $\tilde{H}_2 = H_2 - h$, where $h \in (0, \frac{1}{4})^2$. Next we define a candidate Lyapunov function given by

$$L_2(x_2, y_2) = \frac{1}{2} \tilde{H}_2^2, \quad (28)$$

and note that $L_2 > 0$ for all $\tilde{H}_2 \neq 0$ and that $L_2 = 0$ if and only if $\tilde{H}_2 = 0$, if and only if $(x_2, y_2) \in \gamma_h$, where by γ_h we denote the reference canard cycle, that is

$$\gamma_h = \left\{ (x_2, y_2) \in \mathbb{R}^2 \mid \tilde{H}_2 = 0 \right\}. \quad (29)$$

It follows that

$$L'_2 = -x_2 \exp(-2y_2) \tilde{H}_2 (2\alpha_2 x_2 + \alpha_2^2 + \mu_2^0), \quad (30)$$

where $\mu_2^0 = \mu_2(0, x_2, y_2, \alpha_2)$. Naturally, we want to design μ_2^0 such that $L'_2 < 0$, or at least $L'_2 \leq 0$. We now see that a convenient choice of μ_2^0 is

$$\mu_2^0 = -2\alpha_2 x_2 - \alpha_2^2 + c_1 x_2 \exp(c_2 y_2) \tilde{H}_2, \quad (31)$$

where $c_1 > 0$ and $c_2 \in \mathbb{R}$ are the controller gains. Using (31) we have

$$L'_2 = -c_1 x_2^2 \exp((c_2 - 2)y_2) \tilde{H}_2^2 \leq 0. \quad (32)$$

Note that the previous inequality holds uniformly in c_2 , however a particular choice of c_2 may drastically change the performance of the controller. The relevance of the constant c_2 shall be detailed in section 3.1.2.

²In principle our analysis holds for $h \leq \frac{1}{4}$, but only the considered interval provides canard cycles, which are our main focus. See also section 3.1.2.

By Lasalle's invariance principle [43] we have that, under the controller (31) and $r_2 = 0$, the trajectories of (25) eventually reach the largest invariant set contained in

$$\mathcal{I} = \{(x_2, y_2) \in \mathbb{R}^2 \mid L'_2 = 0\} = \{x_2 = 0\} \cup \{\tilde{H}_2 = 0\} \quad (33)$$

Note, however that $\{x_2 = 0\}$ is generically not invariant for the closed-loop dynamics (25). Indeed, the closed-loop system (25) (restricted to $r_2 = 0$) reads as

$$\begin{aligned} x'_2 &= -y_2 + x_2^2 + c_1 x_2 \exp(c_2 y_2) \tilde{H}_2 \\ y'_2 &= x_2, \end{aligned} \quad (34)$$

where setting $x_2 = 0$ leads to $(x'_2, y'_2) = (-y_2, 0)$. Therefore, we now have that all trajectories of (25) eventually reach $\mathcal{I}_2 = \{(x_2, y_2) = (0, 0)\} \cup \{\tilde{H}_2 = 0\}$. Since the origin is an equilibrium point of (34)³, we have that every trajectory with initial conditions $(x_2(0), y_2(0)) \in \mathbb{R}^2 \setminus \{(0, 0)\}$ eventually reaches the set $\{\tilde{H}_2 = 0\}$ as $t_2 \rightarrow \infty$. With the previous analysis we have shown the following.

Proposition 1. *Consider (25). Then, one can choose constants $c_1 > 0$ and $c_2 \in \mathbb{R}$ such that for $r_2 \geq 0$ sufficiently small a controller of the form*

$$\mu_2 = -2\alpha_2 x_2 - \alpha_2^2 + c_1 x_2 \exp(c_2 y_2) (H_2 - h) + \mathcal{O}(r_2), \quad (35)$$

where H_2 is as in (27), renders the orbit γ_h locally asymptotically stable.

Proof. The proof follows from our previous analysis and regular perturbation arguments. \square

We show in Figure 4 a simulation of the result postulated in Proposition 1.

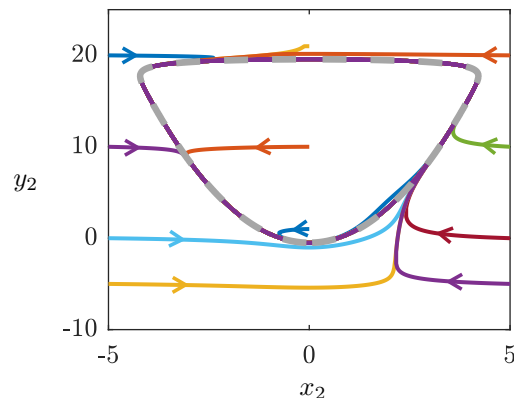


Figure 4: Simulation of (25) with the controller (31). The parameters for the simulation are $(r_2, \alpha_2, c_1, c_2, h) = (0, 1, 1, 2, 1 \times 10^{-16})$. The desired periodic orbit is depicted as the dashed curve.

³In fact it is straightforward to further show that the origin is an unstable equilibrium point of (34).

Let us emphasize at this point that designing the controller in the rescaling chart justifies using H_2 to define a convenient Lyapunov function, even if there are higher order terms in the original vector field (18). We also point out that the maximal canard becomes unbounded in this chart. Such a case shall be studied in chart K_1 (see section 3.1.2 below). Next we digress on how to deal with a certain class of higher order terms even if r_2 is not small.

Lemma 1. *Consider (25) with $r_2 > 0$ fixed and let $\Gamma_2 \subset \mathbb{R}^2$ be a neighbourhood of γ_h . Assume that the function g_2 satisfies*

1. $g_2 = x_2\phi_2(r_2, x_2, y_2, \alpha_2)$, where ϕ_2 is smooth.
2. The function ϕ_2 satisfies $1 + r_2\phi_2(r_2, 0, y_2, \alpha_2) \neq 0$ for all $(0, y_2) \in \Gamma_2$.
3. The function ϕ_2 satisfies $1 + r_2\phi_2(r_2, \gamma_h, \alpha_2) \neq 0$.

Then, one can choose constants $c_1 > 0$ and $c_2 \in \mathbb{R}$ such that a controller of the form

$$\mu_2 = -2\alpha_2 x_2 - \alpha_2^2 + c_1 x_2 \exp(c_2 y_2) (H_2 - h) - (y_2 - x_2^2) r_2 \phi_2 \quad (36)$$

renders γ_h locally asymptotically stable in Γ_2 .

Proof. Similar to the analysis performed above, we consider (25) but now with an extra $\mathcal{O}(r_2)$ -term in the controller, namely

$$\begin{aligned} x_2' &= -y_2 + (x_2 + \alpha_2)^2 + \mu_2^0 + r_2 \nu_2 \\ y_2' &= x_2 + r_2 g_2, \end{aligned} \quad (37)$$

where μ_2^0 is as in (31) and now $\nu_2 = \nu_2(r_2, x_2, y_2, \alpha_2)$ is to be designed. Under the first assumption we write $g_2 = x_2\phi_2$ for some smooth function $\phi_2 = \phi_2(r_2, x_2, y_2, \alpha_2)$. Consider, as before, the candidate Lyapunov function (28). After substituting μ_2^0 we get

$$L_2' = -c_1 x_2^2 \tilde{H}_2^2 \exp((c_2 - 2)y_2) - r_2 x_2 \tilde{H}_2 \exp(-2y_2) (\nu_2 + (y_2 - x_2^2)\phi_2). \quad (38)$$

The above expression suggests to set $\nu_2 = -(y - x_2^2)\phi_2$. By doing so one gets (30) again and therefore, invoking again Lasalle's invariance principle, we now take a look at the set $\mathcal{I} = \{x_2 = 0\} \cup \{\tilde{H}_2 = 0\}$ related to the closed-loop system. To be more precise we now focus on

$$\begin{aligned} x_2' &= -y_2 + x_2^2 + c_1 x_2 \exp(c_2 y_2) \tilde{H}_2 - r_2 (y_2 - x_2^2) \phi_2 \\ y_2' &= x_2 + r_2 x_2 \phi_2, \end{aligned} \quad (39)$$

and consider its dynamics restricted to \mathcal{I} . On $\{x_2 = 0\}$ one has $(x_2', y_2') = (-y_2(1 + r_2\phi_2|_{\{x_2=0\}}), 0)$. Therefore, to avoid $\{x_2 = 0\}$ being invariant we impose the condition $1 + r_2\phi_2(r_2, 0, y_2, \alpha_2) \neq 0$. Note that the aforementioned condition would already suffice to show that trajectories converge towards $\{\tilde{H}_2 = 0\}$, however, there may still be a stable equilibrium point contained in $\{\tilde{H} = 0\}$.

The restriction of (39) to $\{\tilde{H}_2 = 0\}$ reads as

$$\begin{aligned} x_2' &= (-y_2 + x_2^2)(1 + r_2\phi_2) \\ y_2' &= x_2(1 + r_2\phi_2), \end{aligned} \quad (x_2, y_2) \in \gamma_h. \quad (40)$$

Now it suffices to give conditions on $\phi_2|_{\{(x_2, y_2) \in \gamma_h\}}$ such that (40) does not have equilibrium points (keep in mind that $(0, 0) \notin \gamma_h$ for $h \in (0, 1/4)$). Such a condition is simply $1 + r_2\phi_2(r_2, \gamma_h, \alpha_2) \neq 0$, completing the proof. \square

Remark 4.

- If the third assumption of Lemma 1 does not hold, then trajectories converge to an equilibrium point contained in the set $\{\tilde{H}_2 = 0\}$.
- A simpler sufficient condition on ϕ_2 satisfying the hypothesis of Lemma 1 is $\phi_2(r_2, x_2, y_2, \alpha_2) > -1$ for all $(x_2, y_2) \in \Gamma_2$. This is the one we keep for Theorem 1.

We show in Figure 5 a simulation regarding Lemma 1.

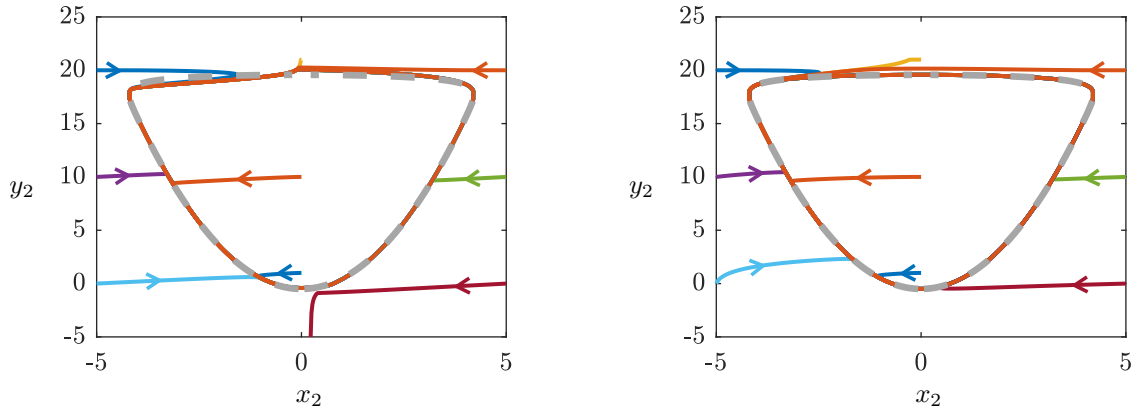


Figure 5: Phase portrait corresponding to (25) with $r_2 = 1$, $\alpha_2 = 1$, $\phi_2 = y_2 - x_2^2$ and $(c_1, c_2) = (10, 2)$. On the left we show the orbits corresponding to $\nu_2 = 0$, and on the right those for ν_2 given as in Lemma 1. Observe on the left that trajectories do not follow the desired canard while on the right they do. This means that the extra term ν_2 is necessary to render the canard asymptotically stable when the perturbations of order $\mathcal{O}(r_2)$ in (25) are not small.

3.1.2 Analysis in the directional chart K_1

We are now going to look at the controlled dynamics in the chart K_1 . This serves two purposes: the first is of giving a more precise meaning to the constant c_2 in the controller (35); the second is to corroborate that the controller designed previously is indeed able to also stabilize the (unbounded) maximal canard. The dynamics in this chart read as

$$\begin{aligned}
 r_1' &= \frac{1}{2}r_1\varepsilon_1(x_1 + r_1\varepsilon_1g_1) \\
 x_1' &= -1 + (x_1 + \alpha_1)^2 - \frac{1}{2}\varepsilon_1x_1^2 + \mu_1 - \frac{1}{2}r_1\varepsilon_1^2g_1 \\
 \varepsilon_1' &= -\varepsilon_1^2(x_1 + r_1\varepsilon_1g_1) \\
 \alpha_1' &= -\frac{1}{2}\varepsilon_1(x_1 + r_1\varepsilon_1g_1).
 \end{aligned} \tag{41}$$

We also have that $H_1 = \kappa_{21}(H_2)$, namely

$$H_1 = \frac{1}{2} \exp(-2\varepsilon_1^{-1}) \left(\varepsilon_1^{-1} - \varepsilon_1^{-1} x_1^2 + \frac{1}{2} \right), \quad (42)$$

and define $\tilde{H}_1 = H_1 - h$. From (35) together with (24) we know that

$$\mu_1 = -2\alpha_1 x_1 - \alpha_1^2 + c_1 \varepsilon_1^{1/2} x_1 \exp(c_2 \varepsilon_1^{-1}) \tilde{H}_1 + \mathcal{O}(r_1 \varepsilon_1^{3/2}). \quad (43)$$

Remark 5.

- μ_1 is bounded along any reference canard $\gamma_h = \{\tilde{H}_1 = 0\}$ with $h \in (0, \frac{1}{4})$.
- If $h \neq 0$, then μ_1 becomes unbounded as $\varepsilon_1 \rightarrow 0$ unless $\tilde{H}_1 = 0$ (previous observation). This is to be expected as, in the limit $\varepsilon_1 \rightarrow 0$ the only canard orbit to stabilize is the maximal canard since $\lim_{\varepsilon_1 \rightarrow 0} H_1 = 0$. Therefore, we are going to study the closed-loop dynamics (41) for the particular choice of $h = 0$ and for the limit $\varepsilon_1 \rightarrow 0$.

So from now on we let $h = 0$, that is $\tilde{H}_1 = H_1 = \frac{1}{2} \exp(-2\varepsilon_1^{-1}) (\varepsilon_1^{-1} - \varepsilon_1^{-1} x_1^2 + \frac{1}{2})$. We also restrict to $\{r_1 = 0\}$. In such a case we have

$$\mu_1 = -2\alpha_1 x_1 - \alpha_1^2 + \frac{1}{2} c_1 \varepsilon_1^{1/2} x_1 \exp((c_2 - 2)\varepsilon_1^{-1}) \left(\varepsilon_1^{-1} - \varepsilon_1^{-1} x_1^2 + \frac{1}{2} \right), \quad (44)$$

and the closed loop system reads as

$$\begin{aligned} x_1' &= -1 + x_1^2 - \frac{1}{2} \varepsilon_1 x_1^2 + \frac{1}{2} c_1 \varepsilon_1^{1/2} x_1 \exp(c_2 \varepsilon_1^{-1}) H_1 \\ \varepsilon_1' &= -\varepsilon_1^2 x_1 \\ \alpha_1' &= -\frac{1}{2} \varepsilon_1 x_1. \end{aligned} \quad (45)$$

It shall also be relevant to consider H_1' , namely

$$\begin{aligned} H_1' &= -\frac{1}{2} c_1 \varepsilon_1^{-1/2} x_1^2 \exp((c_2 - 2)\varepsilon_1^{-1}) H_1 \\ &= -\frac{1}{2} c_1 \varepsilon_1^{-1/2} x_1^2 \exp((c_2 - 4)\varepsilon_1^{-1}) \left(\varepsilon_1^{-1} - \varepsilon_1^{-1} x_1^2 + \frac{1}{2} \right). \end{aligned} \quad (46)$$

First of all we note that, for bounded (x_1, α_1) , we have $\lim_{\varepsilon_1 \rightarrow 0} H_1 = 0$, and $\lim_{\varepsilon_1 \rightarrow 0} H_1' = 0$ for $c_2 < 4$. Next, we focus on (44) where we observe that in order for the controller to be bounded as $\varepsilon_1 \rightarrow 0$ one must choose $c_2 < 2$. To be more precise:

Lemma 2. Consider the controller μ_1 given by (44) and let c_2 be a constant such that for any $K > 0$ one has $c_2 - 2 \leq \varepsilon_1 \ln(K \varepsilon_1^{3/2})$. Then $\lim_{\varepsilon_1 \rightarrow 0} \mu_1 = -2\alpha_1 x_1 - \alpha_1^2$.

Proof. Straightforward computations by substituting $c_2 - 2 \leq \varepsilon_1 \ln(K \varepsilon_1^{3/2})$ in (44). \square

The particularity of Lemma 2 is that it allows one to choose c_2 arbitrarily close to 2 as long as $c_2 < 2$. For all other canards, $c_2 \in \mathbb{R}$ is sufficient. However, $c_2 = 2$ is the appropriate choice as it eliminates the exponential term in (44) and in (46), which is rather convenient for numerical simulations. We remark that a completely analogous analysis, which we omit for brevity, follows for the chart $K_3 = \{\bar{x} = 1\}$ where canards corresponding to $h < 0$ can be considered. The arguments and the conclusion are the same, namely, for $h < 0$ one should set $c_2 < 2$ so that the controller remains bounded along the unbounded canard.

3.1.3 Proof of Theorem 1

To prove Theorem 1 we first blow-down the controller μ_2 . To keep it simple we shall blow-down (35), but of course the same holds for (36). So, recall from (35) that the blown-up controller is

$$\mu_2 = -2\alpha_2 x_2 - \alpha_2^2 + c_1 x_2 \exp(c_2 y_2) (H_2 - h). \quad (47)$$

Next, from (22) we have

$$\hat{u} = \varepsilon \mu_2 = -2\alpha \hat{x} - \alpha^2 + c_1 \hat{x} \varepsilon^{1/2} \exp(c_2 y \varepsilon^{-1}) (\hat{H} - h), \quad (48)$$

where $\hat{H} = \hat{H}(\hat{x}, y, \varepsilon) = \frac{1}{2} \exp(-\frac{2y}{\varepsilon}) \left(\frac{y}{\varepsilon} - \frac{\hat{x}^2}{\varepsilon} + \frac{1}{2} \right)$ as stated in the first item of Theorem 1. Under (48) the closed-loop system corresponding to (18) reads as

$$\begin{aligned} \hat{x}' &= -y + \hat{x}^2 + c_1 \hat{x} \varepsilon^{1/2} \exp(c_2 y \varepsilon^{-1}) (\hat{H} - h) \\ y' &= \varepsilon(\hat{x} + \tilde{g}). \end{aligned} \quad (49)$$

Next, it is important to observe that $\lim_{\varepsilon \rightarrow 0} \hat{H} = 0$. This means that for $\varepsilon = 0$ the only reference canard that is reachable is the maximal canard, which corresponds to $h = 0^4$. So, setting $h = 0$, and since one chooses $c_2 < 2$ (recall Section 3.1.2), it follows that $\lim_{\varepsilon \rightarrow 0} c_1 \hat{x} \varepsilon^{1/2} \exp(c_2 y \varepsilon^{-1}) \hat{H} = 0$, meaning that the layer equation for (49) is

$$\begin{aligned} \hat{x}' &= -y + \hat{x}^2 \\ y' &= 0, \end{aligned} \quad (50)$$

which indeed has the same type of singularity at the origin as the open-loop system, a fold. This shows that (48) is blow-up compatible.

3.2 The slow control problem

In this section we consider the slow-control problem

$$\begin{aligned} x' &= -y + x^2 + f(x, y, \varepsilon, \alpha) \\ y' &= \varepsilon(x - \alpha + g(x, y, \varepsilon, \alpha) + u(x, y, \varepsilon, \alpha)), \end{aligned} \quad (51)$$

where the objective is, as in Section 3.1, to stabilize a prescribed canard γ_h . Due to space constraints, and because the analysis is similar to the one performed in Section 3.1, we only state the relevant result.

⁴As it is expected, the controller becomes unbounded in the limit $\varepsilon \rightarrow 0$ for any other canard, as they do not exist in such a limit.

Theorem 2. Consider (51) and let $\hat{H} = H(x, y, \varepsilon)$ be defined by (11). Then, one can choose constants $c_1 > 0$, $c_2 \in \mathbb{R}$ and $h \leq \frac{1}{4}$ such that a blow-up compatible controller of the form

$$u = \alpha + c_1(y - x^2)\varepsilon^{-1/2} \exp(c_2 y \varepsilon^{-1})(H - h) \quad (52)$$

renders the canard orbit $\gamma_h = \{(x, y) \in \mathbb{R}^2 \mid H = h\}$ locally asymptotically stable for $\varepsilon > 0$ sufficiently small. A convenient choice of controller gain c_2 for the maximal canard is $c_2 \leq 2 + \frac{5}{2} \frac{\varepsilon}{y} \ln\left(K \frac{\varepsilon}{y}\right)$, for some $K > 0$. By convenient we mean that such a choice ensures that the controller remains bounded as $y \rightarrow \infty$.

Remark 6. In (51) one may avoid introducing u by considering α as the controller. Adapting Theorem 2 to such scenario is straightforward.

In Figure 6 we illustrate the statement of Theorem 2.

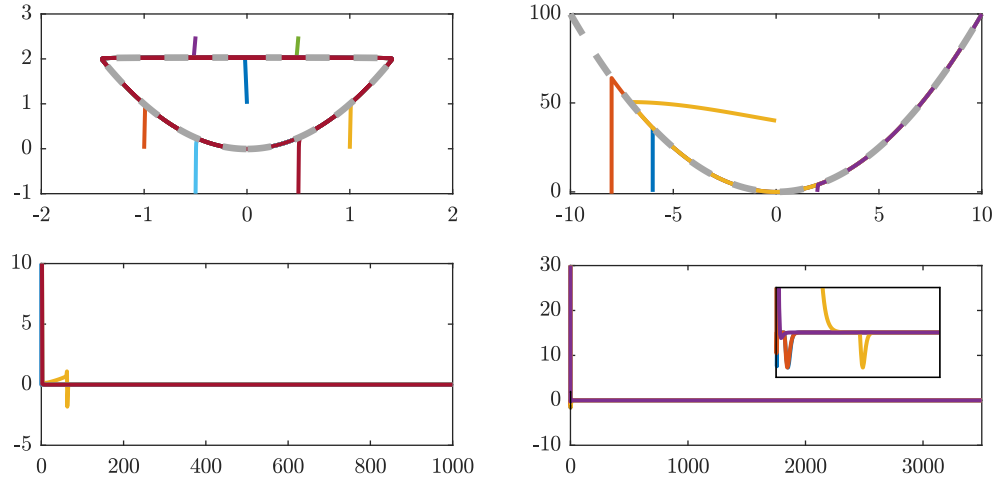


Figure 6: The first column corresponds to the control of a bounded canard cycle (shown in dashed-gray), while the second column to the control of the maximal canard. The first row shows the phase-portrait in (x, y) -coordinates. The second row shows the time series of the corresponding controller. We show on the lower-right diagram a detail of the controller's signal for time close to 0.

4 Controlling Canard Cycles for the van der Pol oscillator

In this section we are going to extend the ideas developed previously to control canard cycles in the van der Pol oscillator. Furthermore, due to its relationship with some neuron models, like the Fitzhugh-Nagumo model [20, 47], we shall consider that the controller acts on the fast variable only. The idea is that the controller represents input current. Thus, let us study

$$\begin{aligned} x' &= -y + x^2 - \frac{1}{3}x^3 + u \\ y' &= \varepsilon x. \end{aligned} \tag{53}$$

Remark 7. *For simplicity, we have chosen to present the case $\alpha = 0$. However, the case $\alpha \neq 0$ follows straightforwardly from considering the arguments at the beginning of Section 3.1.*

System (53) has two fold points, one at the origin and one at $(x, y) = (2, \frac{4}{3})$. In fact, the origin is a canard point and the singular limit of (53) is as shown in Figure 7.

To state our main result, let \mathcal{N}_1 be a neighborhood of the repelling critical manifold \mathcal{S}_0^r and \mathcal{N}_2 a neighborhood of \mathcal{S}_0 around the origin. We assume that such neighborhoods have a nonempty intersection in the first quadrant. Although it is not necessary to be precise on such neighborhoods, since several choices are possible, an example of \mathcal{N}_1 and \mathcal{N}_2 is as follows

$$\begin{aligned} \mathcal{N}_1 &= \left\{ (x, y) \in \mathbb{R}^2 : \left| -y + x^2 - \frac{1}{3}x^3 \right| < \beta_1, 0 < x < 2, y_{\min} < y < y_h \right\} \\ \mathcal{N}_2 &= \left\{ (x, y) \in \mathbb{R}^2 : \left| -y + x^2 \right| < \beta_2, -x_{\min} < x < x_{\max} \right\}, \end{aligned} \tag{54}$$

where $y_{\min} \in \mathcal{O}(\varepsilon)$. Furthermore, let the repelling slow manifold $\mathcal{S}_\varepsilon^r$ be given by the graph of $x = \phi(y, \varepsilon)$.

Proposition 2. *Consider (53) and let ψ_i be a bump function with support \mathcal{N}_i . Then, one can choose \mathcal{N}_i , positive constants c_1 and k_1 , and a small constant x^* , $|x^*| < 1$, such that the controller*

$$u = \frac{1}{2}u_1\psi_1 + \frac{1}{2}u_2\psi_2, \tag{55}$$

where

$$\begin{aligned} u_1 &= -F_0 - F_{x^*} + v_1 \\ u_2 &= c_1 x \varepsilon^{-1/2} \left(y - x^2 + \frac{\varepsilon}{2} \right), \end{aligned} \tag{56}$$

and with

$$\begin{aligned} F_{x^*}(x, y, \varepsilon) &= -y + (x - x^* \sqrt{y})^2 - \frac{(x - x^* \sqrt{y})^2 \varepsilon}{2y} - \frac{1}{3}(x - x^* \sqrt{y})^3 \\ v_1(y, \varepsilon) &= \frac{2\phi + x^* \sqrt{y}}{\phi} \left(-y + \phi^2 - \frac{\varepsilon}{2y} \phi^2 - \frac{1}{3} \phi^3 \right) - \left(\frac{\varepsilon}{y} \phi + \sqrt{y} \phi^2 + k_1 \sqrt{y} \right) (x - \phi - x^* \sqrt{y}), \end{aligned} \tag{57}$$

stabilizes a canard cycle with height y_h . Moreover, if $x^* < 0$ then the canard is without head, while if $x^* > 0$ then the canard is with head.

Sketch of proof: As before, all the analysis is carried-out in the blow-up space. The overall idea is as follows: the controller to be designed acts only within a small neighbourhood of $\{0\} \cup \mathcal{S}_\varepsilon^r$, mainly because the rest of the slow manifold is already stable, so there is no need of stabilizing it. The desired height of the canard is regulated by the constant y_h . The controller in the central chart is as in Section 3.1. In fact, we can choose the constants $h = 2$ and $c_2 = 2$ due to the fact that we want to follow the maximal canard just in a small and bounded domain near the origin. So, the new analysis is performed in the chart $K_1 = \{\bar{y} = 1\}$, where the objective is to stabilize the (normally hyperbolic) repelling branch of the slow manifold $\mathcal{S}_\varepsilon^r$. The most important feature is to control the location of the orbits relative to $\mathcal{S}_\varepsilon^r$ as it is precisely such location that determines the direction of the jump once the orbits reach the desired height. To avoid smoothness issues, the regions where the controllers are active are defined via bump functions. A schematic representation of this idea is provided in Figure 7, while the details of the proof follows from Sections 4.1 and 4.2. \square

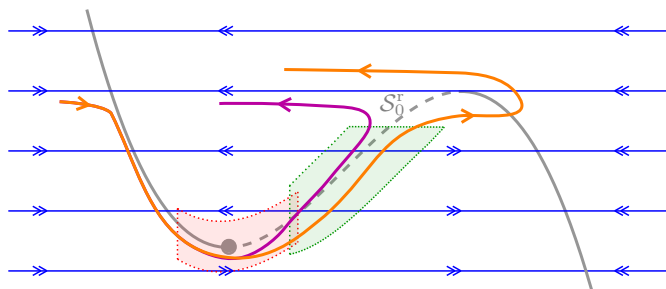
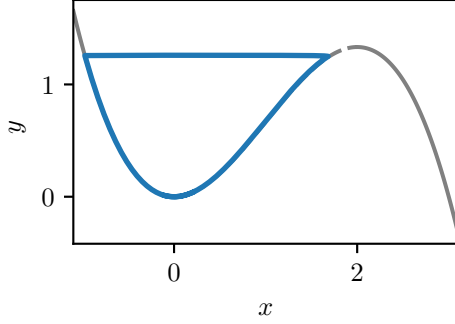


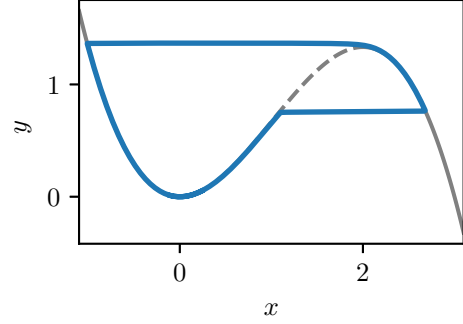
Figure 7: Strategy for the control design: first within a small neighborhood (red-shaded region) of the canard point, we use the controller designed in Section 3. Afterwards, a second controller is designed in chart K_1 and whose task is to stabilize the (normally hyperbolic) repelling branch $\mathcal{S}_\varepsilon^r$. This second controller is active on a neighborhood (green-shaded region) of \mathcal{S}_0^r . Furthermore, it is via such controller that we steer the orbits towards either side of $\mathcal{S}_\varepsilon^r$. This induces that the trajectories jump towards the desired direction once the second controller is inactive. The two orbits illustrate the aforementioned strategy.

In Figure 8 we show some simulations using the proposed controller.

Before proceeding with the proof of Proposition 2, let us point out that it is straightforward to use the proposed controller to produce robust Mixed Mode Oscillations (MMOs) [11]. One way to do this is as follows: first of all, we assume that we are able to count the number of Small Amplitude Oscillations (SAOs) and of Large Amplitude Oscillations (LAOs). Next, let us say that we start by following a canard without head, so we set the controller constant $x^* < 0$ and y_h to the desired height. After the number of desired SAOs has been reached, we change the controller constant x^* to $x^* > 0$ and, if desired, y_h to a new height value. So, the controller will now steer the system to follow a canard with head. This process can be repeated to produce any other pattern allowed by the geometry of the van der Pol oscillator. We show in Figure 9 an example of stable MMOs that one can obtain using the controller of Proposition 2.



(a) A stable canard without head. For this simulation we have set $y_h = 1.25$ and $x^* = -0.01$.



(a) A stable canard with head. For this simulation we have set $y_h = 0.75$ and $x^* = 0.01$.

Figure 8: Numerical simulations illustrating the controller of Proposition 2. In all these simulations we have used $\varepsilon = 0.01$ and $(c_1, k_1) = (1, 1)$.

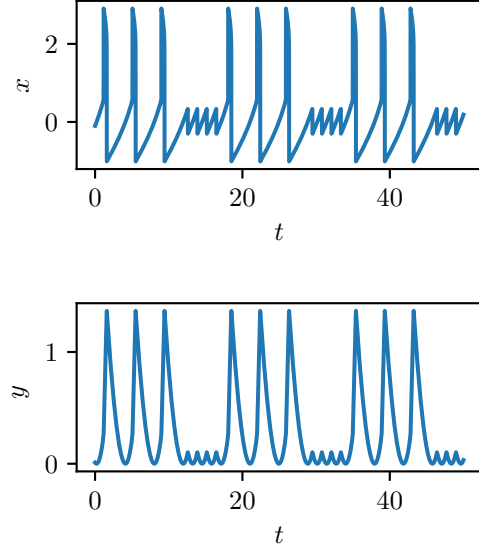
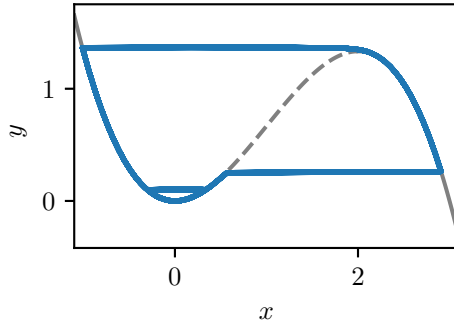


Figure 9: A sample of a Mixed-Mode Oscillation (MMO) with 3 Large Amplitude Oscillations (LAOs) and 4 Small Amplitude Oscillations (SAOs) obtained using the controller of Proposition 2.

4.1 Analysis in the directional chart K_1

Similar to the analysis in section 3.1.2 we use a directional blow-up defined by

$$x = r_1 x_1, \quad y = r_1^2, \quad \varepsilon = r_1^2 \varepsilon_1, \quad u = r_1^2 \mu_1, \quad \alpha = r_1 \alpha_1. \quad (58)$$

Therefore, the local vector field associated to (53) reads as

$$\begin{aligned} r_1' &= \frac{1}{2} r_1 \varepsilon_1 x_1 \\ \varepsilon_1' &= -\varepsilon_1^2 x_1 \\ x_1' &= -1 + x_1^2 - \frac{1}{2} x_1^2 \varepsilon_1 - \frac{1}{3} r_1 x_1^3 + \mu_1. \end{aligned} \quad (59)$$

To have a better idea of what we are going to achieve with the controller, it is worth to first look at the uncontrolled dynamics.

Let us define a domain

$$D_1 = \{(r_1, \varepsilon_1, x_1) \in \mathbb{R}^3 \mid 0 \leq r_1 \leq \rho_1, 0 \leq \varepsilon_1 \leq \delta_1, x_1 \in \mathbb{R}\}. \quad (60)$$

Lemma 3. *Consider (59) with $\mu_1 = 0$. Then, one can choose constants $\rho_1 > 0$ and $\delta_1 > 0$ such that the following properties hold within the domain D_1 .*

1. *There exist semi-hyperbolic equilibrium points $p_{1,\pm} = (r_1, \varepsilon_1, x_1) = (0, 0, \pm 1)$. The point $p_{1,-}$ is attracting while $p_{1,+}$ is repelling along the x_1 -axis.*
2. *Let \mathcal{M}_1 be defined by*

$$\mathcal{M}_1 = \left\{ (r_1, \varepsilon_1, x_1) \in \mathbb{R}^3 \mid \varepsilon_1 = 0, r_1 = 3 \left(\frac{1}{x_1} - \frac{1}{x_1^3} \right) \right\}. \quad (61)$$

The set \mathcal{M}_1 corresponds to the set of equilibrium points of (59) restricted to $\{\varepsilon_1 = 0\}$. Moreover, let us denote the subsets

$$\begin{aligned} \mathcal{M}_{1,-} &= \{(r_1, \varepsilon_1, x_1) \in \mathcal{M}_1 \mid x_1 < 0\}, \\ \mathcal{M}_{1,+} &= \{(r_1, \varepsilon_1, x_1) \in \mathcal{M}_1 \mid x_1 \geq 1\}. \end{aligned} \quad (62)$$

The subset $\mathcal{M}_{1,-}$ is attracting and the subset $\mathcal{M}_{1,+}$ can be partitioned as $\mathcal{M}_{1,+} = \mathcal{M}_{1,+}^r \cup \left\{ \left(\frac{3-\sqrt{3}}{\sqrt{3}}, 0, \sqrt{3} \right) \right\} \cup \mathcal{M}_{1,+}^a$ where

$$\begin{aligned} \mathcal{M}_{1,+}^r &= \left\{ (r_1, \varepsilon_1, x_1) \in \mathcal{M}_{1,+} \mid 1 \leq x_1 < \sqrt{3} \right\}, \\ \mathcal{M}_{1,+}^a &= \left\{ (r_1, \varepsilon_1, x_1) \in \mathcal{M}_{1,+} \mid x_1 > \sqrt{3} \right\} \end{aligned} \quad (63)$$

are the repelling and attracting branches of $\mathcal{M}_{1,+}$, respectively.

3. *Restricted to $\{r_1 = 0\}$ there exist 1-dimensional local center manifolds $\mathcal{E}_{1,-}$ and $\mathcal{E}_{1,+}$ located, respectively, at the points $p_{1,-}$ and $p_{1,+}$. Such manifolds are given by*

$$\mathcal{E}_{1,\pm} = \{(r_1, \varepsilon_1, x_1) \in \mathbb{R}^3 \mid r_1 = 0, x_1 = h_{1,\pm}(\varepsilon_1)\}, \quad (64)$$

where

$$h_{1,\pm}(\varepsilon_1) = \pm \left(1 + \frac{\varepsilon_1}{2}\right)^{1/2}. \quad (65)$$

The flow along $\mathcal{E}_{1,-}$ is directed away from the point $p_{1,-}$ and the flow along $\mathcal{E}_{1,+}$ is directed towards the point $p_{1,+}$. Furthermore, the center manifolds $\mathcal{E}_{1,\pm}$ are unique.

4. There exist 2-dimensional local centre manifolds $\mathcal{W}_{1,\pm}$ that contain, respectively, the point $p_{1,\pm}$, the branch of equilibrium points $\mathcal{M}_{1,\pm}$ and the centre manifold $\mathcal{E}_{1,\pm}$. These centre manifolds are unique and, moreover, $\mathcal{W}_{1,-}$ is attracting and $\mathcal{W}_{1,+}$ is repelling.

Sketch of the proof, see [39] for details. The first two items are obtained by straightforward computations. The expression of the centre manifolds follow from the fact that the restriction of (4.1) to $\{r_1 = 0\}$ has the invariant (just as in the fold case) $H_1 = \frac{1}{2} \exp(-2\varepsilon_1^{-1}) (\varepsilon_1^{-1} - \varepsilon_1^{-1} x_1^2 + \frac{1}{2})$. Therefore the functions $h_{1,\pm}$ are given by the solutions of $H_1 = 0$. The flow on $\mathcal{E}_{1,\pm}$ follows from the equation $\varepsilon_1' = -\varepsilon_1^2 x_1$. The uniqueness of $\mathcal{E}_{1,\pm}$ is due to the fact that $p_{1,\pm}$ is a semi-hyperbolic saddle of the dynamics of (59) restricted to $\{r_1 = 0\}$. Finally, the existence and properties of $\mathcal{W}_{1,\pm}$ follow from local analysis at $p_{1,\pm}$, centre manifold theory, the previous arguments, and by choosing $\rho_1 < \frac{3-\sqrt{3}}{\sqrt{3}}$. The previous choice of ρ_1 is particularly necessary for the stability property of $\mathcal{W}_{1,+}$. \square

Remark 8. $\mathcal{W}_{1,+}$ is related, via the blow-up map, to $\mathcal{S}_\varepsilon^+$. Therefore, the task of the controller is going to be to stabilize the centre manifold $\mathcal{W}_{1,+}$.

Remark 9. In what follows, we are going to define some geometric objects, in particular centre manifolds, for the closed-loop dynamics. To make a clear distinction between their open-loop counterparts, and to be able to compare them, we shall denote relevant geometric objects of the closed-loop system by a cl superscript.

In this section we are going to be interested only in $(x_1, \varepsilon_1) \in \mathbb{R}_+^2$. So, to simplify notation let

$$h_1^{\text{cl}}(\varepsilon_1) = h_{1,+}(\varepsilon_1) = \left(1 + \frac{\varepsilon_1}{2}\right)^{1/2}. \quad (66)$$

Furthermore, let us assume that the centre manifold $\mathcal{W}_{1,+}$ (recall Lemma 3) is given by the graph of

$$x_1 = \phi_1(r_1, \varepsilon_1). \quad (67)$$

Note that $\phi_1(0, \varepsilon_1) = h_1^{\text{cl}}(\varepsilon_1)$. Therefore, one can in fact write

$$\phi_1(r_1, \varepsilon_1) = h_1^{\text{cl}}(\varepsilon_1) + \sum_{\substack{i \geq 1 \\ j \geq 0}} \sigma_{ij} r_1^i \varepsilon_1^j, \quad (68)$$

for some coefficients $\sigma_{ij} \in \mathbb{R}$. We now proceed with the following steps.

1. *Reverse the direction of the flow in the x_1 -direction:* Define $f_1(r_1, \varepsilon_1, x_1) = -1 + x_1^2 - \frac{1}{2}x_1^2\varepsilon_1 - \frac{1}{3}r_1x_1^3$ and let $\mu_1 = -f_1(r_1, \varepsilon_1, x_1) - f_1(r_1, \varepsilon_1, x_1 - x_1^*) + \nu_1$, where $x_1^* \sim 0$ is a constant (the

usefulness of x_1^* will become evident below) and $\nu_1 = \nu_1(r_1, \varepsilon_1, x_1)$ is to be further designed. With this step we have that (59) now reads as

$$\begin{aligned} r_1' &= \frac{1}{2}r_1\varepsilon_1x_1 \\ \varepsilon_1' &= -\varepsilon_1^2x_1 \\ x_1' &= -f_1(r_1, \varepsilon_1, x_1 - x_1^*) + \nu_1. \end{aligned} \tag{69}$$

2. *Design ν_1 so that (69) has $\mathcal{W}_1^{\text{cl}} := \{(r_1, \varepsilon_1, r_1) \in \mathbb{R}^3 \mid x_1 = x_1^* + \phi_1(r_1, \varepsilon_1)\}$ as a closed-loop centre manifold:* this step requires standard centre manifold computations. By performing them we find that

$$\nu_1 = \frac{2\phi_1 + x_1^*}{\phi_1} \left(-1 + \phi_1^2 - \frac{1}{2}\phi_1^2\varepsilon_1 - \frac{1}{3}r_1\phi_1^3 \right). \tag{70}$$

Note that, if we restrict to $\{r_1 = 0\}$, (69) now reads as

$$\begin{aligned} \varepsilon_1' &= -\varepsilon_1^2x_1 \\ x_1' &= 1 - (x_1 - x_1^*)^2 + \frac{1}{2}(x_1 - x_1^*)^2\varepsilon_1 + \varepsilon_1^2 \frac{2h_1^{\text{cl}} + x_1^*}{4h_1^{\text{cl}}}. \end{aligned} \tag{71}$$

We know that (71) has a centre manifold $\mathcal{E}_1^{\text{cl}} := \{(\varepsilon_1, x_1) \in \mathbb{R}_{\geq 0}^2 \mid x_1 = x_1^* + h_1^{\text{cl}}(\varepsilon_1)\}$. Furthermore, it follows from straightforward computations that the equilibrium point $p_1^* := (0, 0, 1 + x_1^*)$ is attracting along the x_1 -axis. This means that $\mathcal{E}_1^{\text{cl}}$, and also $\mathcal{W}_1^{\text{cl}}$, are locally (near p_1^*) attracting. Next we improve such stability.

3. *Design a variational controller that renders $\mathcal{W}_1^{\text{cl}}$ locally exponentially stable:* For this it is enough to take the x_1 -component of the variational equation. So, let $z_1 = x_1 - \phi_1 - x_1^*$. The corresponding variational equation along $\mathcal{W}_1^{\text{cl}}$ is

$$z_1' = (-2 + \varepsilon_1 + r_1\phi_1)\phi_1z_1. \tag{72}$$

Recall from (68) that $\phi_1 > 0$ for $r_1 \geq 0$ sufficiently small. Then, we propose to introduce in (72) a variational controller $w_1(\varepsilon_1, z_1)$ of the form

$$w_1 = -(\varepsilon_1\phi_1 + r_1\phi_1^2 + k_1)z_1, \tag{73}$$

where $k_1 \geq 0$. With w_1 as above, the closed-loop variational equation becomes

$$z_1' = -(2\phi_1 + k_1)z_1, \tag{74}$$

and we readily see that, for $r_1 \geq 0$ sufficiently small, $z_1 \rightarrow 0$ exponentially as $t_1 \rightarrow \infty$ (where by t_1 we denote the time-parameter in this chart). We also notice that the constant k_1 helps to improve the contraction rate towards $\mathcal{W}_1^{\text{cl}}$. Moreover, since w_1 vanishes along $\mathcal{W}_1^{\text{cl}}$, the variational controller does not change the closed-loop centre manifold $\mathcal{W}_1^{\text{cl}}$. Finally, observe that the role of the small constant x_1^* is to shift the position of $\mathcal{W}_1^{\text{cl}}$ relative to its open-loop counterpart $\mathcal{W}_{1,+}$. This is important in order to tune the direction along which the trajectory jumps once the controller is inactive.

4. *Restrict next to $\{\varepsilon_1 = 0\}$:* Note that $\nu_1(r_1, 0, x_1) = 0$, then we have

$$\begin{aligned} r_1' &= 0 \\ \varepsilon_1' &= 0 \\ x_1' &= -f_1(r_1, 0, x_1 - x_1^*). \end{aligned} \tag{75}$$

Similar to the previous step, the new line of equilibrium points is slightly shifted according to x_1^* . In fact, the relevant set of stable equilibrium points of (75) is given as

$$\mathcal{M}_1^{\text{cl}} = 3 \left\{ (r_1, \varepsilon_1, x_1) \in \mathbb{R}^3 \mid \varepsilon_1 = 0, r_1 = 3 \left(\frac{1}{x_1 - x_1^*} - \frac{1}{(x_1 - x_1^*)^3} \right), r_1 < \frac{2}{\sqrt{3}} \right\}. \tag{76}$$

Linearization of (75) along $\mathcal{M}_1^{\text{cl}}$ shows that $\mathcal{M}_1^{\text{cl}}$ is exponentially attracting in the x_1 -direction. Therefore, we can conclude that $\mathcal{W}_1^{\text{cl}}$ is located at $x_1 = 1 + x_1^*$, and that it contains the exponentially attracting centre manifold $\mathcal{E}_1^{\text{cl}}$ and the curve of exponentially attracting equilibrium points $\mathcal{M}_1^{\text{cl}}$.

5. Note that the flow along the centre manifold $\mathcal{W}_1^{\text{cl}}$ has not changed and is given, up to smooth equivalence and away from its corner at $x_1 = 1 + x_1^*$, by

$$\begin{aligned} r_1' &= \frac{1}{2}r_1 \\ \varepsilon_1' &= -\varepsilon_1. \end{aligned} \tag{77}$$

In other words, the flow along $\mathcal{W}_1^{\text{cl}}$ is of saddle type.

With the previous steps we can now prove the main result of this section. For this, let us define the domain $D_1^+ = D_1|_{x_1 \geq 0}$ and the sections

$$\begin{aligned} \Sigma_1^{\text{en}} &= \{ (r_1, \varepsilon_1, x_1) \in D_1^+ \mid \varepsilon_1 = \delta_1 \}, \\ \Sigma_1^{\text{ex}} &= \left\{ (r_1, \varepsilon_1, x_1) \in D_1^+ \mid r_1 = \rho_1, 0 < \rho_1 < \frac{2}{\sqrt{3}} \right\}. \end{aligned} \tag{78}$$

Also, define a small rectangle

$$R_1 = \{ (r_1, \varepsilon_1, x_1) \in \Sigma_1^{\text{en}} \mid |x_1 - h_1^{\text{cl}} - x_1^*| \leq \sigma_1, r_1 \leq \tilde{\rho}_1 < \rho_1 \}, \tag{79}$$

Proposition 3. *Consider (59) with the controller*

$$\mu_1 = -f_1(r_1, \varepsilon_1, x_1) - f_1(r_1, \varepsilon_1, x_1 - x_1^*) + \nu_1(\varepsilon_1, x_1), \tag{80}$$

where

$$\begin{aligned} f_1(r_1, \varepsilon_1, x_1) &= -1 + x_1^2 - \frac{1}{2}x_1^2\varepsilon_1 - \frac{1}{3}r_1x_1^3, \\ \nu_1(\varepsilon_1, x_1) &= \frac{2\phi_1 + x_1^*}{\phi_1} \left(-1 + \phi_1^2 - \frac{1}{2}\phi_1^2\varepsilon_1 - \frac{1}{3}r_1\phi_1^3 \right) - (\varepsilon_1\phi_1 + r_1\phi_1^2 + k_1)(x_1 - x_1^* - \phi_1), \end{aligned} \tag{81}$$

and the function $\phi_1(r_1, \varepsilon_1)$ is defined by the open-loop centre manifold $\mathcal{W}_{1,+}$. Then, one can choose sufficiently small constants $(\delta_1, \rho_1, \sigma_1, \tilde{\rho}_1)$ such that the following hold for the closed-loop system.

1. D_1^+ is forward invariant under the flow of (59).
2. The centre manifold $\mathcal{W}_1^{\text{cl}}$ is locally exponentially attracting for $r_1 \geq 0$ sufficiently small, $\varepsilon_1 \geq 0$ sufficiently small and for $r_1^2 \varepsilon_1 \geq 0$ sufficiently small.
3. If $x_1^* = 0$, the centre manifolds $\mathcal{W}_1^{\text{cl}}$ and $\mathcal{W}_{1,+}$ coincide. On the other hand, if $x_1^* < 0$ (resp. if $x_1^* > 0$) then $\mathcal{W}_1^{\text{cl}}$ is located “to the left” (resp. “to the right”) of $\mathcal{W}_{1,+}$ in the x_1 -direction.
4. The image of R_1 under the flow of (59) is a wedge-like region at $\Sigma_1^{\text{ex}} \cap \mathcal{M}_1^{\text{cl}}$.

Proof. The proof follows directly from our previous analysis. In particular, the second item is implied by the stability properties of $\mathcal{W}_1^{\text{cl}}|_{\{r_1=0\}}$, $\mathcal{W}_1^{\text{cl}}|_{\{\varepsilon_1=0\}}$, and the fact that $r_1^2 \varepsilon_1 = \varepsilon$. \square

The closed-loop dynamics corresponding to (59) under the controller (80) are as sketched in Figure 10.

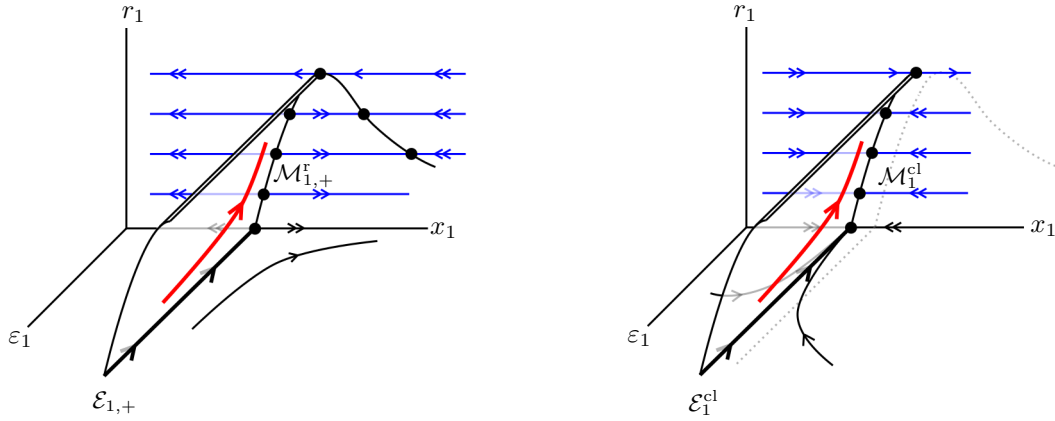


Figure 10: On the left we show the qualitative behavior of the open-loop (that is with $\mu_1 = 0$) system (59), while on the right we show the closed-loop system obtained with the controller of Proposition 3. In both cases, the 2-dimensional surface illustrates the centre manifolds $\mathcal{W}_{1,+}$ on the left and $\mathcal{W}_1^{\text{cl}}$. The relative position of $\mathcal{W}_1^{\text{cl}}$ with respect to $\mathcal{W}_{1,+}$ is determined by x_1^* . In the sketch on the right we show that $\mathcal{W}_1^{\text{cl}}$ is to the left of $\mathcal{W}_{1,+}$, which is indicated by the dashed curves.

To finalize this section, we blow-down the controller of Proposition 3, as it will be used in the forthcoming section.

Lemma 4. *Let u_1 denote the blow-down of μ_1 . Then*

$$u_1 = -F_0 - F_{x_1^*} + v_1, \quad (82)$$

where

$$\begin{aligned}
F_{x_1^*}(x, y, \varepsilon) &= -y + (x - x_1^* \sqrt{y})^2 - \frac{(x - x_1^* \sqrt{y})^2 \varepsilon}{2y} - \frac{1}{3}(x - x_1^* \sqrt{y})^3 \\
v_1(y, \varepsilon) &= \frac{2\phi + x_1^* \sqrt{y}}{\phi} \left(-y + \phi^2 - \frac{\varepsilon}{2y} \phi^2 - \frac{1}{3} \phi^3 \right) \\
&\quad - \left(\frac{\varepsilon}{y} \phi + \sqrt{y} \phi^2 + k_1 \sqrt{y} \right) (x - \phi - x_1^* \sqrt{y}),
\end{aligned} \tag{83}$$

and where $\phi = \phi(y, \varepsilon)$ is defined by $\mathcal{S}_\varepsilon^r$, that is by $\mathcal{S}_\varepsilon^r = \{x = \phi(y, \varepsilon)\}$.

Proof. The expression of u_1 follows from straightforward computations using (58) in (80). To check that ϕ is as stated, note that the blow-down induces the relation $\{x_1 = \phi_1\} \leftrightarrow \{x = \sqrt{y} \Phi(\phi_1) = \phi\}$, where by $\Phi(\phi_1)$ we are denoting the blow-down of ϕ_1 . \square

4.2 Composite controller and proof of Proposition 2

In this section we gather the controllers designed in the central chart K_2 and in the directional chart K_1 into a single one. Our arguments follow from the next general design methodology.

1. Let us start with an open-loop vector field $X : \mathbb{R}^N \rightarrow \mathbb{R}^N$ such that $X(0) = 0$ (here possible parameters $\lambda \in \mathbb{R}^p$ are already included in the vector field by the trivial equation $\dot{\lambda} = 0$).
2. Let $\mathcal{B} = \mathbb{S}^{N-1} \times \mathcal{I}$ where \mathbb{S} is the unit sphere and $\mathcal{I} \subseteq \mathbb{R}$ is an interval that contains the origin. Here we shall be interested in $\mathcal{I} = [0, r_0]$, $r_0 > 0$. Recall that the blow-up map is defined as $\Phi : \mathcal{B} \rightarrow \mathbb{R}^N$. Moreover, the blow-up transformation induces the so-called “blown-up” vector field \bar{X} , which is the vector field that makes the following diagram commute.

$$\begin{array}{ccc}
\mathcal{B} & \xrightarrow{\Phi} & \mathbb{R}^N \\
\bar{X} \downarrow & & \downarrow X \\
T\mathcal{B} & \xrightarrow{D\Phi} & T\mathbb{R}^N
\end{array}$$

In other words, \bar{X} and X are related by the push-forward of \bar{X} by Φ , that is $\Phi_*(\bar{X}) = X$, in the sense $D\Phi \circ \bar{X} = X \circ \Phi$ ⁵.

3. Let $\mathcal{A} = \{(K_i, \Phi_i)\}$, with $i = 1, \dots, M$, be a smooth atlas of \mathcal{B} . This means that (K_i, Φ_i) is a chart of \mathcal{B} , the open sets K_i cover \mathcal{B} , and $\Phi_i : K_i \subset \mathcal{B} \rightarrow \mathbb{R}^N$ is a diffeomorphism. Then, there are local vector fields \bar{X}_i defined on K_i and given by $\bar{X}_i = D\Phi_i^{-1} \circ X \circ \Phi_i$.

⁵Recall that \bar{X} is well defined: for $r > 0$ because of $\Phi|_{\{r>0\}}$ being a diffeomorphism, and on $r = 0$ due to continuous extension to the origin, see [40]. Moreover, if the origin is nilpotent, one defines the *desingularized vector field* $\tilde{X} = \frac{1}{r^k} \bar{X}$ for some $k > 0$, which is smoothly equivalent to \bar{X} for $r > 0$, and all the forthcoming arguments hold equivalently for \tilde{X} .

4. On each chart K_i , let us introduce a local controller \bar{u}_i , and define as $\bar{X}_i^{\text{cl}} := \bar{X}_i + \bar{u}_i$ the local closed-loop vector field. Naturally, \bar{u}_i is a local vector field on K_i .
5. Let $\bar{\psi}_i : K_i \rightarrow \mathbb{R}$ be a bump function with compact support $\bar{\mathcal{N}}_i \subset K_i$. We choose each $\bar{\mathcal{N}}_i$ such that if $K_i \cap K_j \neq \emptyset$ then $\bar{\mathcal{N}}_i \cap \bar{\mathcal{N}}_j \neq \emptyset$ as well. Note that

$$\bar{\varphi}_i := \frac{\bar{\psi}_i}{\sum_{i=1}^M \bar{\psi}_i} \quad (84)$$

is a partition of unity subordinate to the open cover $\{K_i\}_{i=1}^M$.

6. The sum

$$\bar{u} := \sum_{i=1}^M \bar{\varphi}_i \bar{u}_i \quad (85)$$

is, by virtue of the partition of unity, well defined as a global controller on \mathcal{B} . Therefore, the global closed-loop vector field $\bar{X}^{\text{cl}} := \bar{X} + \bar{u}$ is also well defined.

7. Let us now blow-down \bar{X}^{cl} . To be more precise, we now define the closed-loop vector field X^{cl} on \mathbb{R}^N by $\Phi_*(\bar{X}^{\text{cl}}) = X^{\text{cl}}$. So, we have

$$X^{\text{cl}} = \Phi_*(\bar{X}^{\text{cl}}) = \Phi_*(\bar{X} + \bar{u}) = \Phi_*(\bar{X}) + \Phi_*(\bar{u}) = X + \Phi_*(\bar{u}), \quad (86)$$

where we have used the fact that the push-forward is linear [44]. Next we define $u := \Phi_*(\bar{u})$ and compute

$$\begin{aligned} u = \Phi_*(\bar{u}) &= \Phi_* \left(\sum_{i=1}^M \bar{\varphi}_i \bar{u}_i \right) = \sum_{i=1}^M \Phi_*(\bar{\varphi}_i \bar{u}_i) = \sum_{i=1}^M (\Phi_i)_*(\bar{\varphi}_i \bar{u}_i) \\ &= \sum_{i=1}^M \varphi_i \cdot (\Phi_i)_*(\bar{u}_i), \end{aligned} \quad (87)$$

where $\varphi_i := \bar{\varphi}_i \circ \Phi_i^{-1}$ for $i = 1, \dots, M$, and it is clear from its definition that $\{\varphi_i\}$ is a partition of unity a neighborhood of the origin $0 \in \mathbb{R}^N$ subordinate to the open cover $\{\Phi_i(K_i)\}$.

With the previous methodology we define the controller that stabilizes canard cycles of the van der Pol oscillator as

$$u = \frac{1}{2} \psi_1 u_1 + \frac{1}{2} \psi_2 u_2, \quad (88)$$

where u_1 is as given by Lemma 4 and u_2 as in Theorem 1, and where ψ_1 is a bump function with support \mathcal{N}_1 containing the repelling branch \mathcal{S}_0^r and \mathcal{N}_2 the parabola $\{y = x^2\}$ around the origin. As an example one can propose

$$\begin{aligned} \mathcal{N}_1 &= \left\{ (x, y) \in \mathbb{R}^2 : \left| -y + x^2 - \frac{1}{3}x^3 \right| < \beta_1, 0 < x < 2, y_{\min} < y < y_h \right\} \\ \mathcal{N}_2 &= \left\{ (x, y) \in \mathbb{R}^2 : \left| -y + x^2 \right| < \beta_2, -x_{\min} < x < x_{\max} \right\}, \end{aligned} \quad (89)$$

with suitably chosen positive constants $\beta_1, \beta_2, x_{\min}, x_{\max}, y_{\min}, y_{\max}$. We note that one must choose $y_{\min} \in \mathcal{O}(\varepsilon)$ in order to ensure that the slow manifold $\mathcal{S}_\varepsilon^r$ is within distance $\mathcal{O}(\varepsilon)$ of the

critical manifold \mathcal{S}_0^* . Here y_h controls the height of the desired canard cycle. The neighborhood \mathcal{N}_1 and \mathcal{N}_2 are sketched in Figure 7.

With the controller as in (88), and given the analysis in Section 4.1, one has that orbits of (53) passing close to the origin follow closely the repelling branch of the slow manifold $\mathcal{S}_\varepsilon^r$ up to a height determined by y_h . Once orbits leave the neighborhood $\mathcal{N}_1 \cup \mathcal{N}_2$, they are governed by the open-loop dynamics. Finally the controller of Proposition 2 is indeed (88). We have just dropped the subscript of the constant x_1^* .

5 Conclusions and Outlook

In this paper we have presented a methodology that combines the blow-up method with Lyapunov-based control techniques to design a controller that stabilizes canard cycles. The main idea is that in the blow-up space one can use a first integral to regulate the canard cycle that the orbits are to follow. Later on, we have extended the previously developed method to control canard cycles in the van der Pol oscillator. Roughly speaking this procedure follows two steps: first one needs a controller that stabilizes a folded maximal canard within a small neighborhood of the canard point. Next, one needs to stabilize the unstable branch of the open-loop slow manifold and to tune the position of the closed-loop orbits with respect to it. This is essential to determine whether the closed-loop canard has a head or not. Finally one combines such controllers by means of a partition of unity. We have further showed that the proposed controller can be used to produce stable MMOs.

Several new questions and possible extensions arise from our work, and we would like to finish this paper by briefly mentioning a couple of ideas. First of all, it becomes interesting to adapt the controllers designed here to neuron models such as the FitzHugh-Nagumo, Morris-Lecar, or Hodgkin-Huxley models. Another relevant extension is to develop optimal controllers to control canards. Although from a theoretical point of view one would be interested in arbitrary cost functionals, some particular choices might be more suitable for applications. For instance, one may want to design minimal energy controllers. It is also not completely clear whether the strategy of combining the blow-up method and control techniques still applies as the optimal controllers may be time-dependent. Finally, the notion of controlling MMOs definitely requires further investigation, as here we have just given a simple sample of the possibilities. Thus, for example, extending the ideas of this paper to 3-dimensional fast-slow systems with a folded critical manifold is a direction to be pursued in the future.

References

- [1] V. I. Arnol'd, A. N. Varchenko, and S. M. Gusein-Zade. *Singularities of Differentiable Maps: Volume I : Classification of Critical Points, Caustics and Wave Fronts*. Springer Science & Business Media, 2012.
- [2] Z. Artstein. Asymptotic stability of singularly perturbed differential equations. *Journal of Differential Equations*, 262(3):1603 – 1616, 2017.
- [3] Z. Artstein. Invariance principle in the singular perturbations limit. *Discrete & Continuous Dynamical Systems - B*, 24:3653, 2019.

- [4] Z. Artstein and V. Gaitsgory. Tracking fast trajectories along a slow dynamics: A singular perturbations approach. *SIAM Journal on Control and Optimization*, 35(5):1487–1507, 1997.
- [5] Z. Artstein and A. Leizarowitz. Singularly perturbed control systems with one-dimensional fast dynamics. *SIAM Journal on Control and Optimization*, 41(2):641–658, 2002.
- [6] J. Banasiak and M. Lachowicz. *Methods of small parameter in mathematical biology*. Springer, 2014.
- [7] E. Benoît. Chasse au canard. *Collectanea Mathematica*, 31-32(1-3):37–119, 1981.
- [8] E. Benoît. Canards et enlacements. *Publications Mathématiques de l’Institut des Hautes Études Scientifiques*, 72(1):63–91, 1990.
- [9] M. Brøns and K. Bar-Eli. Canard explosion and excitation in a model of the belousov-zhabotinskii reaction. *The Journal of Physical Chemistry*, 95(22):8706–8713, 1991.
- [10] Joe H Chow, G Peponides, PV Kokotovic, B Avramovic, and JR Winkelman. *Time-scale modeling of dynamic networks with applications to power systems*, volume 46. Springer, 1982.
- [11] M. Desroches, J. Guckenheimer, B. Krauskopf, C. Kuehn, H. M. Osinga, and M. Wechselberger. Mixed-mode oscillations with multiple time scales. *SIAM Review*, 54(2):211–288, 2012.
- [12] M. G. Dmitriev and G. A. Kurina. Singular perturbations in control problems. *Automation and Remote Control*, 67(1):1–43, 2006.
- [13] Florian Dorfler and Francesco Bullo. Synchronization and transient stability in power networks and nonuniform kuramoto oscillators. *SIAM Journal on Control and Optimization*, 50(3):1616–1642, 2012.
- [14] F. Dumortier and R. Roussarie. *Canard cycles and center manifolds*, volume 577. American Mathematical Society, 1996.
- [15] J. Durham and J. Moehlis. Feedback control of canards. *Chaos: An Interdisciplinary Journal of Nonlinear Science*, 18(1):015110, 2008.
- [16] W. Eckhaus. *Matched asymptotic expansions and singular perturbations*, volume 6. Elsevier, 2011.
- [17] G. B. Ermentrout and D. H. Terman. *Mathematical foundations of neuroscience*, volume 35. Springer Science & Business Media, 2010.
- [18] N. Fenichel. Persistence and smoothness of invariant manifolds for flows. *Indiana University Mathematics Journal*, 21(3):193–226, 1971.
- [19] N. Fenichel. Geometric singular perturbation theory for ordinary differential equations. *Journal of differential equations*, 31(1):53–98, 1979.
- [20] R. FitzHugh. Mathematical models of excitation and propagation in nerve. *Biological engineering*, pages 1–85, 1969.
- [21] E. Fridman. A descriptor system approach to nonlinear singularly perturbed optimal control problem. *Automatica*, 37:543–549, 2001.

- [22] E. Fridman. State-feedback h control of nonlinear singularly perturbed systems. 2001.
- [23] E. Hairer and G. Wanner. *Solving Ordinary Differential Equations II: Stiff and Differential-Algebraic Problems*, volume 14. Springer, 2010.
- [24] G. Hek. Geometric singular perturbation theory in biological practice. *Journal of mathematical biology*, 60(3):347–386, 2010.
- [25] E. M. Izhikevich. *Dynamical systems in neuroscience*. MIT press, 2007.
- [26] H. Jardón-Kojakhmetov and C. Kuehn. A survey on the blow-up method for fast-slow systems. *arXiv preprint arXiv:1901.01402*, 2019.
- [27] H. Jardón-Kojakhmetov, M. Muñoz-Arias, and J. M. A. Scherpen. Model reduction of a flexible-joint robot: a port-hamiltonian approach. *IFAC-PapersOnLine*, 49(18):832–837, 2016.
- [28] H. Jardón-Kojakhmetov and J. M. A. Scherpen. Model Order Reduction and Composite Control for a Class of Slow-Fast Systems Around a Non-Hyperbolic Point. *IEEE Control Systems Letters*, 1(1):68–73, 2017.
- [29] H. Jardón-Kojakhmetov, J. M. A. Scherpen, and D. del Puerto-Flores. Stabilization of a class of slow-fast control systems at non-hyperbolic points. *Automatica*, 99:13–21, 2019.
- [30] C. K. R. T. Jones. Geometric singular perturbation theory. In *Dynamical Systems*, pages 44–118. Springer, 1995.
- [31] Hans G Kaper, Tasso J Kaper, and Antonios Zagaris. Geometry of the computational singular perturbation method. *Mathematical modelling of natural phenomena*, 10(3):16–30, 2015.
- [32] T. J. Kaper. An introduction to geometric methods and dynamical systems theory for singular perturbation problems. In *Analyzing Multiscale Phenomena Using Singular Perturbation Methods*, volume 56, pages 85–131. American Mathematical Soc., 1999.
- [33] J. K. Kevorkian and J. D. Cole. *Multiple scale and singular perturbation methods*, volume 114. Springer Science & Business Media, 2012.
- [34] P. Kokotović, H. K. Khalil, and J. O’Reilly. *Singular perturbation methods in control: analysis and design*, volume 25. SIAM, 1999.
- [35] P. V. Kokotović. Applications of singular perturbation techniques to control problems. *SIAM review*, 26(4):501–550, 1984.
- [36] P. V. Kokotović, J. J. Allemon, J. R. Winkelman, and J. H. Chow. Singular perturbation and iterative separation of time scales. *Automatica*, 16(1):23–33, 1980.
- [37] P. V. Kokotović, R. E. O’Malley Jr, and P. Sannuti. Singular perturbations and order reduction in control theoryan overview. *Automatica*, 12(2):123–132, 1976.
- [38] M. Krupa and P. Szmolyan. Extending geometric singular perturbation theory to nonhyperbolic points—fold and canard points in two dimensions. *SIAM journal on mathematical analysis*, 33(2):286–314, 2001.

- [39] M. Krupa and P. Szmolyan. Relaxation oscillation and canard explosion. *Journal of Differential Equations*, 174(2):312–368, 2001.
- [40] C. Kuehn. *Multiple time scale dynamics*, volume 191. Springer, 2015.
- [41] P. Kunkel and V. Mehrmann. *Differential-algebraic equations: analysis and numerical solution*, volume 2. European Mathematical Society, 2006.
- [42] G. A. Kurina, M. G. Dmitriev, and D. S. Naidu. Discrete singularly perturbed control problems (a survey). *Dynamics of Continuous, Discrete and Impulsive Systems Series B: Applications and Algorithms*, 24(5):335–370, 2017.
- [43] J. LaSalle. Some extensions of Liapunov’s second method. *IRE Transactions on circuit theory*, 7(4):520–527, 1960.
- [44] J. M. Lee. Smooth manifolds. In *Introduction to Smooth Manifolds*, pages 1–31. Springer, 2013.
- [45] E. F. Mishchenko and N. Kh. Rozov. *Differential equations with small parameters and relaxation oscillations*. Springer, 1980.
- [46] J. Moehlis. Canards in a Surface Oxidation Reaction. *Journal of Nonlinear Science*, 12(4):319–345, 2002.
- [47] J. Nagumo, S. Arimoto, and S. Yoshizawa. An active pulse transmission line simulating nerve axon. *Proceedings of the IRE*, 50(10):2061–2070, 1962.
- [48] D. S. Naidu. Singular perturbations and time scales in control theory and applications: an overview. *Dynamics of Continuous Discrete and Impulsive Systems Series B*, 9:233–278, 2002.
- [49] D. S. Naidu and A. J. Calise. Singular perturbations and time scales in guidance and control of aerospace systems: A survey. *Journal of Guidance, Control, and Dynamics*, 24(6):1057–1078, 2001.
- [50] R. E. O’Malley, Jr. *Singular perturbation methods for ordinary differential equations*, volume 89 of *Applied Mathematical Sciences*. Springer-Verlag, New York, 1991.
- [51] J. A. Sanders, F. Verhulst, and J. A. Murdock. *Averaging methods in nonlinear dynamical systems*, volume 59. Springer, 2007.
- [52] B. Siciliano and W. J. Book. A singular perturbation approach to control of lightweight flexible manipulators. *The International Journal of Robotics Research*, 7(4):79–90, 1988.
- [53] M. W. Spong. Control of flexible joint robots: a survey. *Coordinated Science Laboratory Report no. UILU-ENG-90-2203, DC-116*, 1990.
- [54] F. Takens. Constrained equations; a study of implicit differential equations and their discontinuous solutions. In *Structural stability, the theory of catastrophes, and applications in the sciences*, pages 143–234. Springer, 1976.
- [55] F. Verhulst. *Methods and applications of singular perturbations: boundary layers and multiple timescale dynamics*, volume 50. Springer Science & Business Media, 2005.

- [56] M. Wechselberger. A propos de canards. *Transactions of the American Mathematical Society*, 364(6):3289–3309, 2012.